

Impact of Scattering on the Strained Ge Nanowire pFETs

Jieyu Qin^{1,2}, Jingjie Zhang^{1,2}, Gang Du², Xiaoyan Liu^{2,*}
¹Shenzhen Graduate School, Peking University, Guangdong 518055, China
²Institute of Microelectronics, Peking University, Beijing 100871, China
 *Email: xyliu@ime.pku.edu.cn

1. Introduction

With the down-scaling of the CMOS devices, Gate-All-Around (GAA) Ge p-channel devices have been drawing a lot of interest not only due to their excellent suppression of the short channel effects (SCEs) and good achievement of ON-current but also due to their high hole mobility [1]. It has been reported that lattice mismatch strain and mechanism stress is induced into channel due to the high-k dielectric and metal gate respectively [2~3]. The hole mobility which is related with acoustic phonon scattering, optical phonon scattering and surface roughness scattering [4], will unavoidably be affected by strain induced in the channel. In this work, the performance of the strained GAA Ge nanowire (NW) pFETs are investigated including the quasi-ballistic transport [5], the effects of lattice mismatch strain and mechanism stress on the performance of Ge NW pFETs are also evaluated. The results are important to optimize and develop model for Ge NW FETs.

2. Device Structure and Simulation Method

The device structure is as shown in Fig. 1. The radius of the cylinder Ge NW is 5nm, and the thickness of the high-k dielectric (HfO₂) is 3nm. The axial direction of the Ge NW is (110), which is same with the carriers' transport direction from the source to the drain (the z-axis). The continuum elastic model and the 6×6 *k*·*p* method are employed to calculate the strain distribution and the valence band structure respectively [4] [6]. The acoustic phonon scattering (ac), optical phonon scattering (op) and surface roughness (sr) scattering are included in the hole mobility calculation [4]. Finally, the quasi-ballistic model based on the backscattering is used to evaluate the I-V characteristics of the Ge NW pFETs [5]. The effects of different scattering mechanisms (ac, op and sr) on the performance of strained Ge NW pFETs are compared.

3. Results and Discussion

Fig. 2 shows the strain tensor component distribution in the Ge NW with 3nm HfO₂ gate dielectric and the same Ge NW under 0.5GPa boundary force. The lattice mismatch between germanium and HfO₂ leads to compressive ε_{zz} in the Ge NW, but the boundary force eliminates the compressive ε_{zz} slightly as shown in Fig. 2(c). Fig. 3(b) shows the valence band structure of the Ge NW with HfO₂. Compared with the pure Ge NW shown in Fig. 3(a), the lattice mismatch strain up-shifts and warps the valence band remarkably. However, less subbands up-shifting is observed in the Ge NW with boundary force as shown in Fig. 3(c). It originates from the smaller compressive ε_{zz} in the NW which leads to less band-up-shifting.

Fig. 4 plots the hole mobility in Ge NWs with different scattering mechanisms under different effective electric fields. The hole mobility degenerates with the increasing effective electric fields. Larger hole mobility degradation at higher effective electric fields is observed when both

phonon and surface roughness scattering are considered. It is because the surface-roughness-limited mobility is strongly dependent on the effective electric fields. The hole mobility in the strained Ge NWs is much larger than that of the pure Ge NWs. It can be understood by the smaller hole effective masses in the strained devices as shown in Fig. 5.

Fig. 6 and Fig. 7 show the I_{DS}-V_{GS} and the I_{DS}-V_{DS} characteristics of the Ge NW with HfO₂ under different scattering mechanisms respectively. The surface roughness scattering leads to larger drain current degradation at higher |V_{GS}| as shown in both Fig. 6 and Fig. 7. This is because surface roughness scattering leads to larger mobility decrement with increasing |V_{GS}|, and the degraded mobility leads to a smaller mean-free-path and higher backscattering coefficient according to eq. (1).

$$r = \frac{l}{l + \lambda_0} \quad (1)$$

Where λ_0 is the mean-free-path; *l* is the critical length which is the gate length in the linear region and the width of the “*kT*-layer” in the saturated region. The same phenomenon is observed in the device with 0.5GPa boundary force as shown in Fig. 8. Table I summarizes the ON-currents of different Ge NW pFETs with different scattering mechanisms and ΔI_{ON} is the degradation caused by surface roughness scattering. The surface roughness scattering results in approximately 30% I_{ON} reduction in strained devices and 36% decrement in unstrained ones. Moreover, the boundary force also leads to current degradation due to the smaller band-up-shifting. Fig. 9 shows the backscattering coefficient of the devices with HfO₂ as a function of gate length under different drain bias. The backscattering coefficient becomes lower with shrinking gate length and higher drain bias.

4. Conclusions

The effects of phonon- and surface-roughness-limited hole mobility and the performance of strained Ge NW pFETs are investigated in this work. The performance of the devices is degraded due to the surface roughness scattering and about 30% I_{ON} decrement is observed in strained device. The boundary force also degrades the device current. The backscattering coefficient decreases with smaller gate length and higher drain bias.

Acknowledgement

This research is supported by NKBRP 2011CBA00604 and 2009ZX02305-003.

References

- [1] Y. Huang and C. Lieber, *Pure Appl. Chem.*, **76**(2004)2051.
- [2] H. Xu, and X. Liu, et al., *IEEE Transactions on Nanotechnology*, **10**(2011)1126.
- [3] D. Wang, and Q. Wang, et al., *Appl. Phys. Lett.*, **83**(2003) 2432.
- [4] M. Fischetti and Z. Ren, et al., *J. Appl. Phys.* **94** (2003) 1079.
- [5] M. Lundstrom, *IEEE Electron Device Lett.* **22**(2001) 293.
- [6] L. Landau, et al., *Theory of elasticity*, Oxford, UK, 1986.

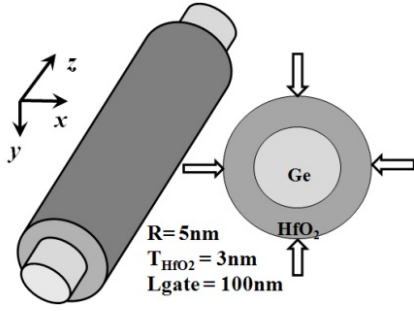


Fig. 1: The Ge nanowire structure.

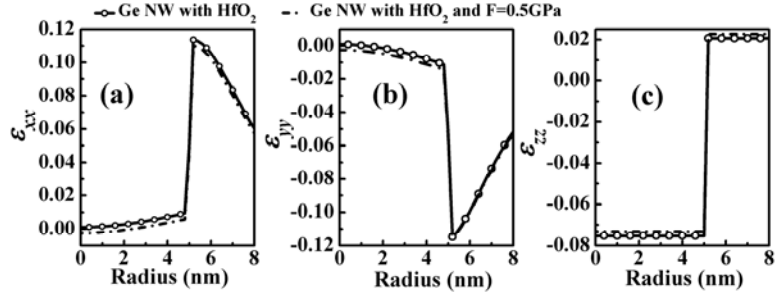


Fig. 2: The strain tensor component distribution along the x -axis.

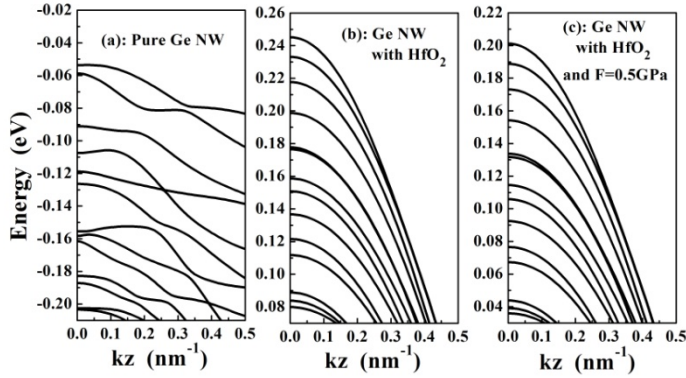


Fig. 3: The valence band structure of different (110) Ge NWs. (a): Pure Ge NW; (b): Ge NW with HfO₂; (c): Ge NW with HfO₂ and 0.5GPa boundary stress.

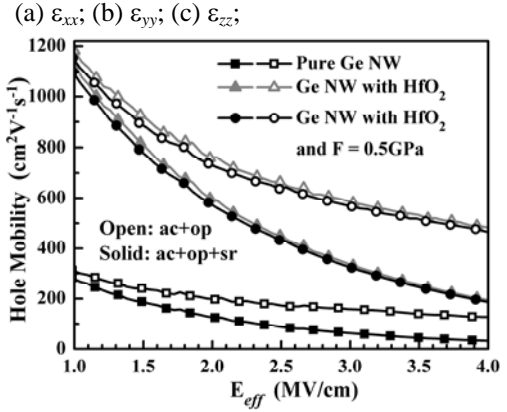


Fig. 4: The effective hole mobility in different (110) Ge NWs with different scattering mechanisms.

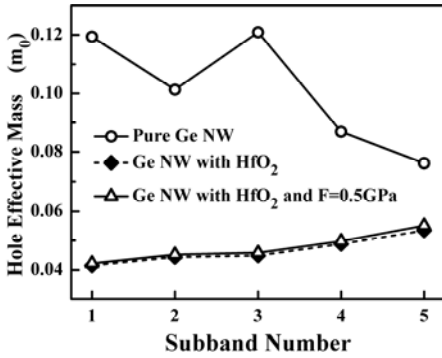


Fig. 5: The effective hole masses of the top five subbands in different Ge NWs.

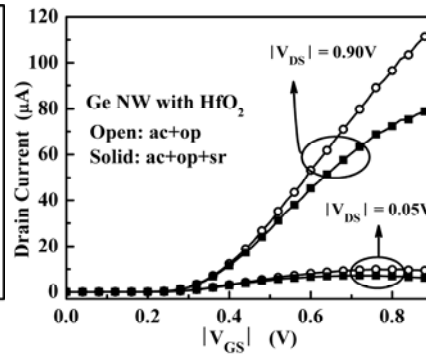


Fig. 6: The I_{DS} - V_{GS} characteristics of Ge NW pFETs with HfO₂.

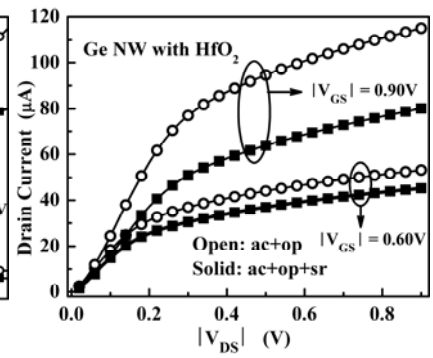


Fig. 7: The I_{DS} - V_{DS} characteristics of Ge NW pFETs with HfO₂.

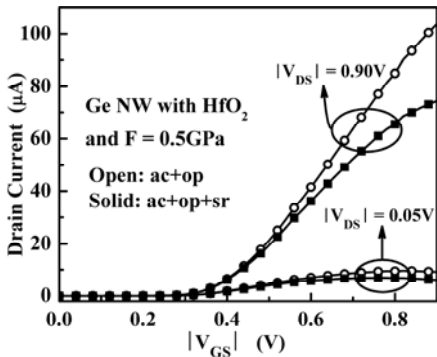


Fig. 8: The I_{DS} - V_{GS} characteristics of Ge NW pFETs with HfO₂ and F=0.5GPa.

Type	ON-Current (μA)		ΔI_{ON}
	ac+op	ac+op+sr	
(a)	25.9	16.5	-36.3%
(b)	115.0	80.1	-30.3%
(c)	103.9	74.5	-28.3%

The ON-Current of different Ge NW pFETs with different scattering mechanisms. (a) Pure Ge NW; (b) Ge NW with HfO₂; (c) Ge NW with HfO₂ and F=0.5GPa. $|V_{GS}| = |V_{DS}| = 0.90\text{V}$.

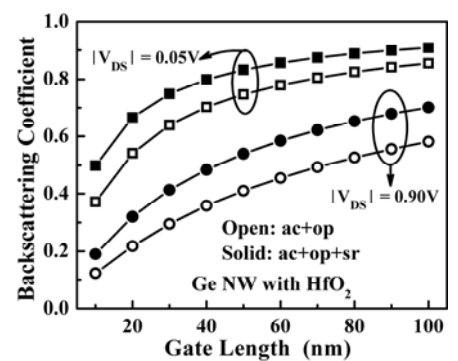


Fig. 9: The backscattering coefficient of Ge NW pFETs with HfO₂. $|V_{GS}| = 0.90\text{V}$.